Integration of Multi-scale Defects for Optimizing Thermoelectric Properties of N-Type $Cu_{1-x}Cd_xFeS_2$ (x=0-0.1)

Bangzhi Ge[1], Jiabin Hu[1], Zhongqi Shi[1, *], Hailong Wang[3], Hongyan Xia[1], Guanjun Qiao[1, 2]

[1] State Key Laboratory for Mechanical Behavior of Materials, Xi'an Jiaotong University, Xi'an 710049, China

[2] School of Materials Science and Engineering, Jiangsu University, Zhenjiang 212013, China

[3] Advanced Energy Storage Materials and Devices Lab, School of Physics and Electronic-Electrical Engineering, Ningxia University, Yinchuan, 750021, China

Supporting Information:

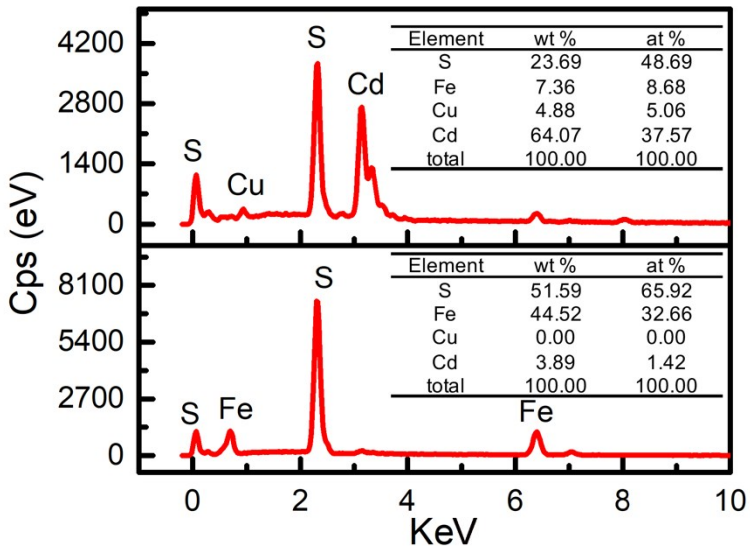

Figure S1. EDS results of (a) CdS precipitates (white area) and (b) the FeS_2 precipitates (gray area) in Figure 2. (d)

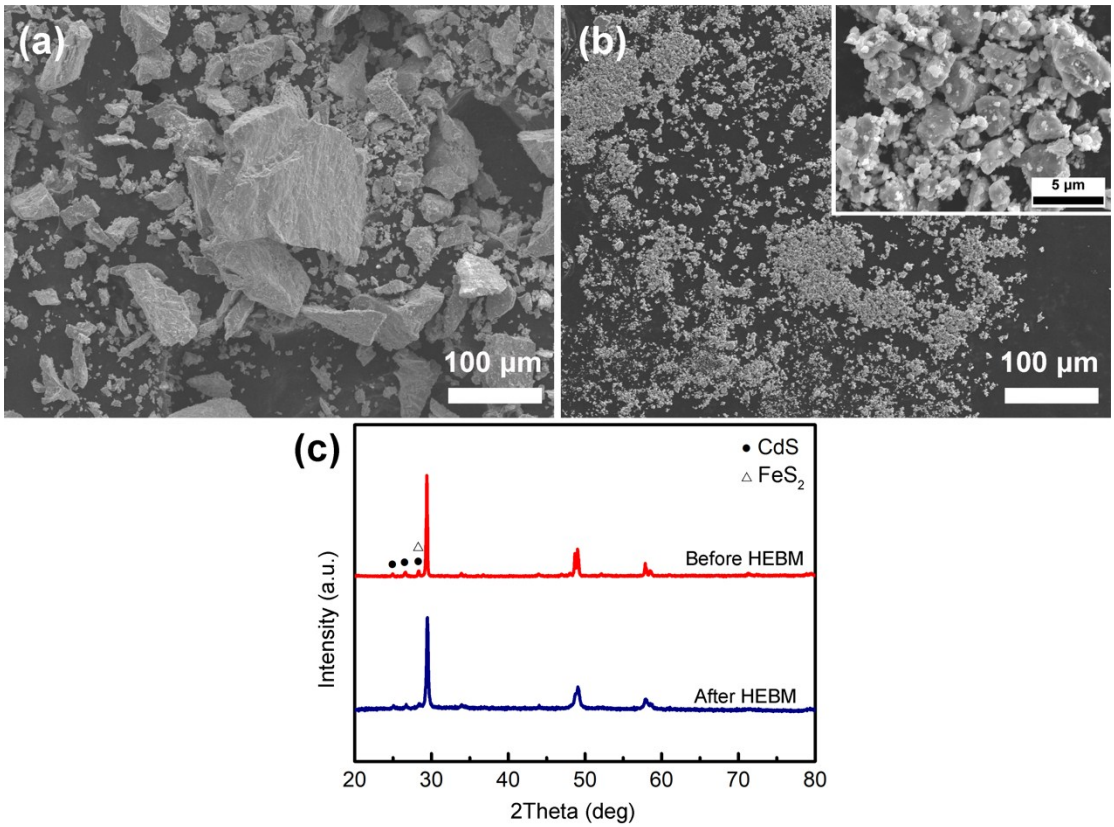

Figure S2. The SEM images of the $Cu_{0.92}Cd_{0.08}FeS_2$ powders (a) berfore and (b) after HEBM, and (c) the corresponding XRD patterns.

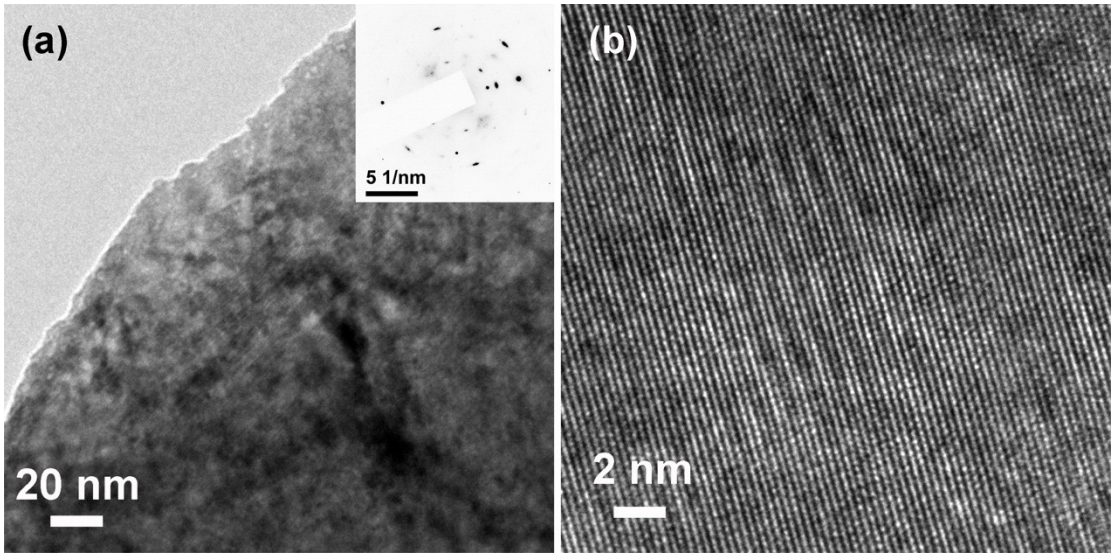

Figure S3. (a) The TEM image of $Cu_{0.92}Cd_{0.08}FeS_2$ with SAED pattern, and (b) the corresponding HRTEM image.

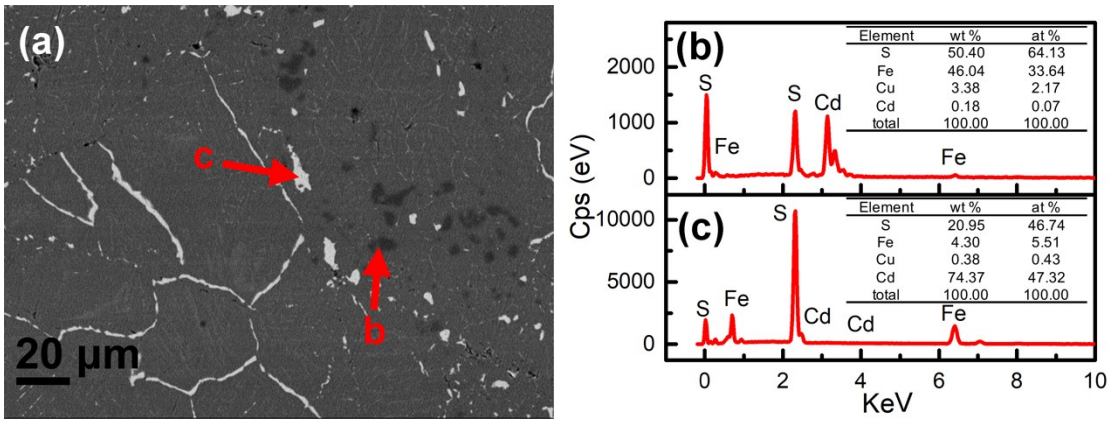

Figure S4. The BSE images of $Cu_{0.92}Cd_{0.08}FeS_2$ sample prepared by quenching and annealing without high-energy ball milling process (a), the EDS result of b point (b) and c point (c).

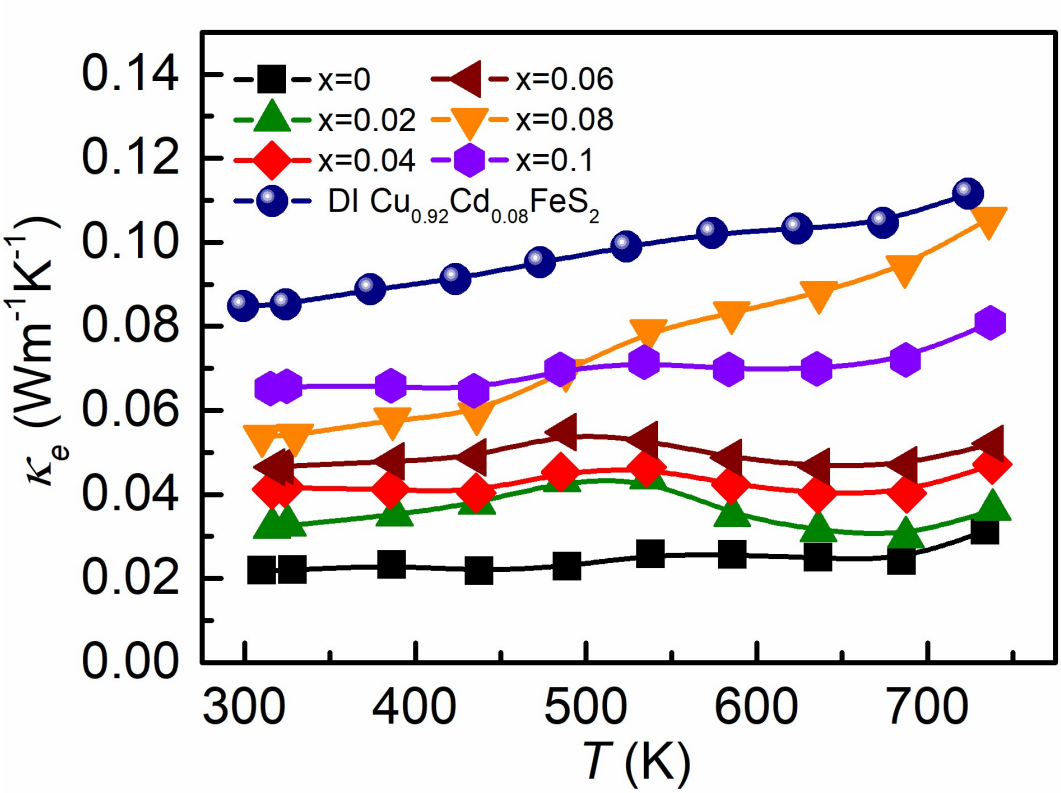

Figure S5. The electron thermal conductivity (k_e) of $Cu_{0.92}Cd_{0.08}FeS_2$ (red circulars) and defects integrated $Cu_{0.92}Cd_{0.08}FeS_2$ (blue squares) samples.

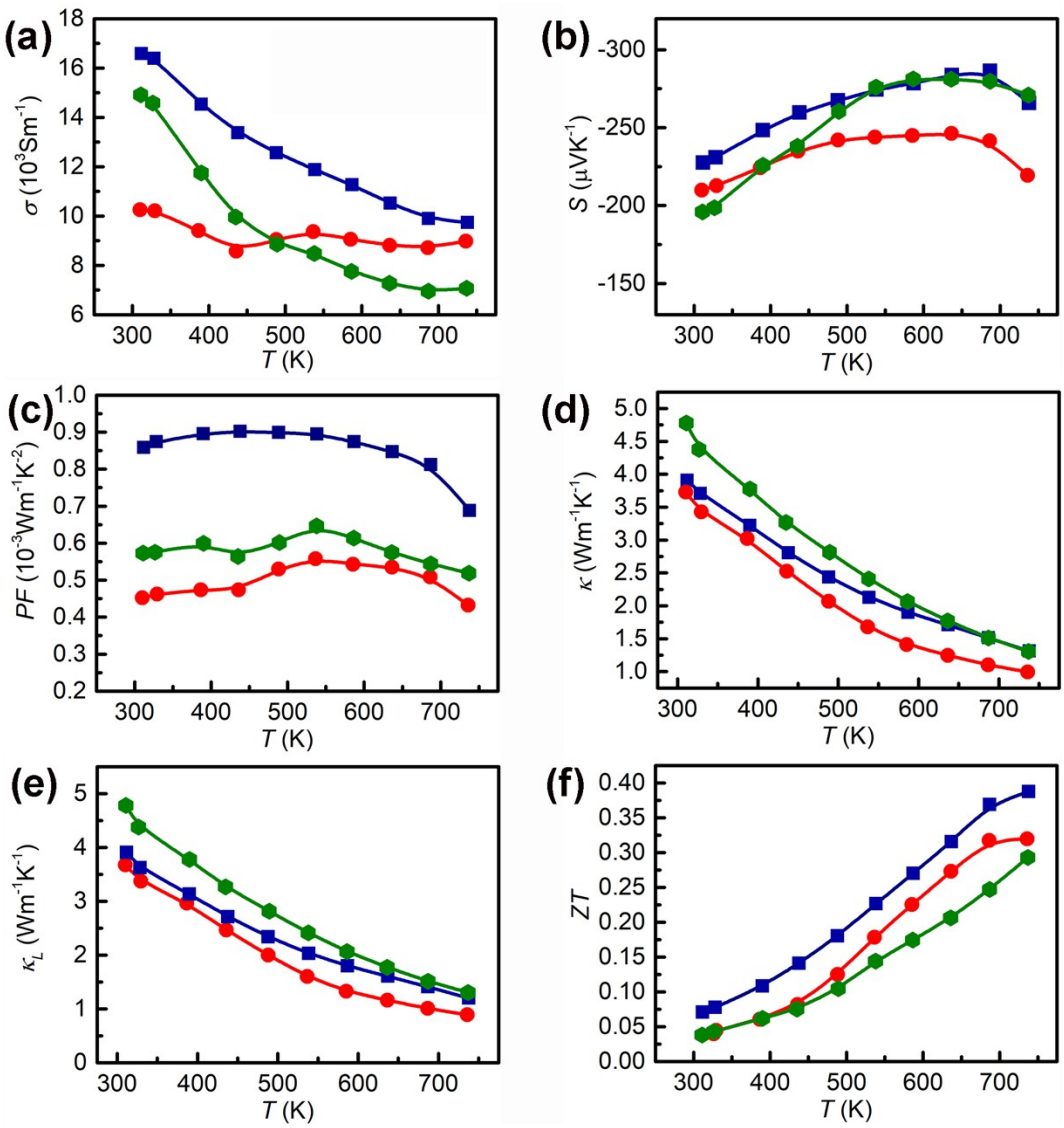

Figure S6. The (a) electrical conductivity (σ), (b) Seebeck coefficient (S), (c) power factor (PF), (d) electronic thermal conductivity (k), (e) lattic thermal conductivity (k_l) and estimated theory k_l, and (f) figure of merit (ZT) of the $Cu_{0.92}Cd_{0.08}FeS_2$ (red circulars), defects integrated $Cu_{0.92}Cd_{0.08}FeS_2$ (blue squares) and $Cu_{0.92}Cd_{0.08}FeS_2$ sample prepared by quenching and annealing without high-energy ball milling process (green hexagon).

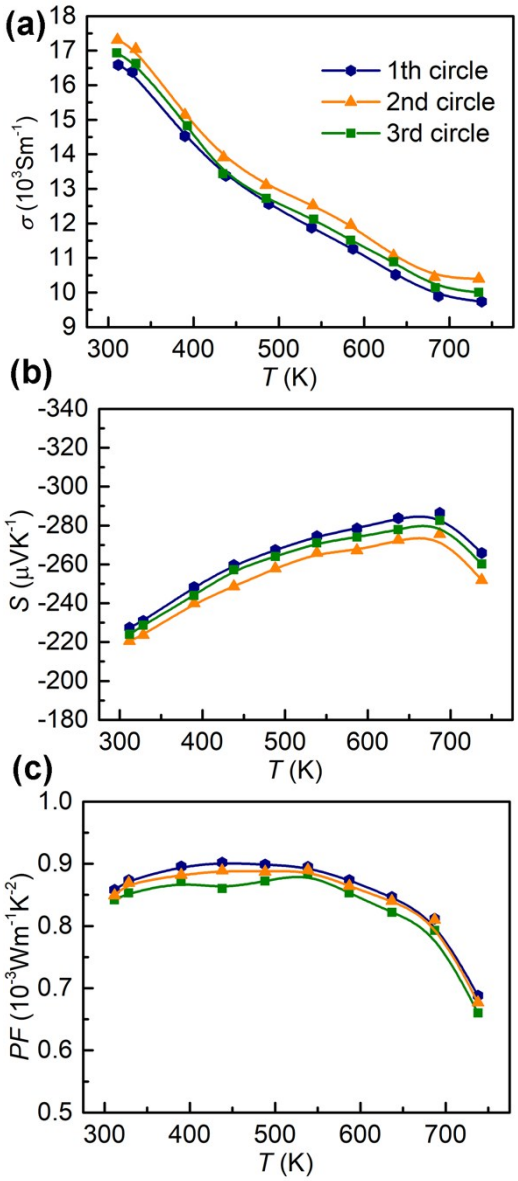

Figure S7. The (a) electrical conductivity (σ), (b) Seebeck coefficient (S), (c) power factor (PF) of cycle testing

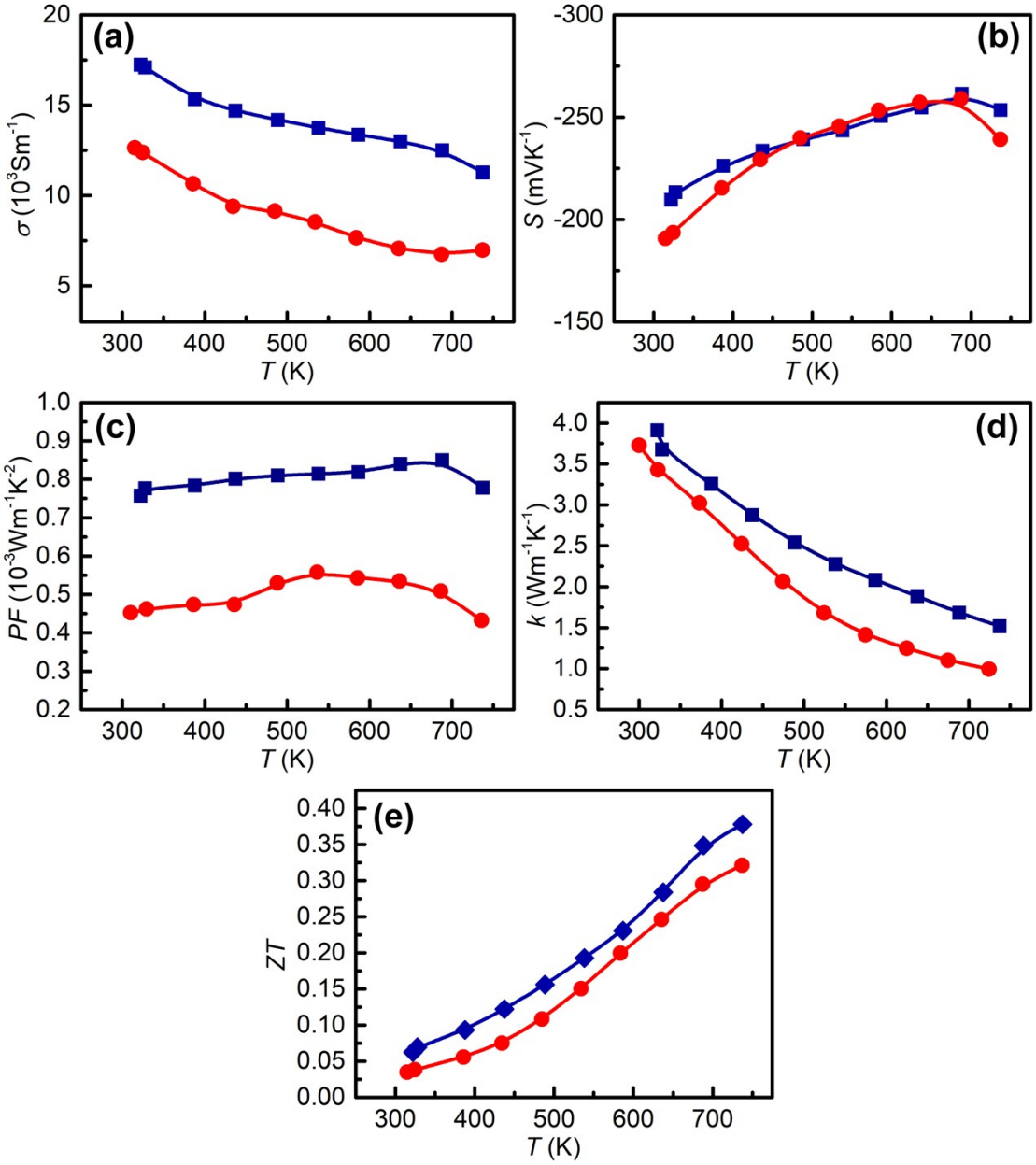

Figure S8. The (a) electrical conductivity (σ), (b) Seebeck coefficient (S), (c) power factor (PF), (d) electronic thermal conductivity (k), and (e) figure of merit (ZT) of the $Cu_{0.9}Cd_{0.1}FeS_2$ (red circulars) and DI-$Cu_{0.9}Cd_{0.1}FeS_2$ (blue squares) samples.

Table S1. The density of all the samples

Sample	Density (g/cm³)
$CuFeS_2$	4.09
$Cu_{0.98}Cd_{0.02}FeS_2$	4.05
$Cu_{0.96}Cd_{0.04}FeS_2$	4.04
$Cu_{0.94}Cd_{0.06}FeS_2$	4.07
$Cu_{0.92}Cd_{0.08}FeS_2$	4.06
$Cu_{0.90}Cd_{0.1}FeS_2$	4.02
DI-$Cu_{0.92}Cd_{0.08}FeS_2$	4.10

Theoretical calculation of scattering parameter (Γ)[1, 2]:

$$\Gamma_{mass} = \frac{\sum_{a=1}^{n} c_a \left(\frac{\bar{M}_a}{\bar{\bar{M}}}\right) f_a^1 f_a^2 \left(\frac{M_a^1 - M_a^2}{\bar{M}_a}\right)^2}{\sum_{a=1}^{n} c_a} \tag{S1}$$

$$\Gamma_s = \frac{\sum_{a=1}^{n} c_a \left(\frac{\bar{M}_a}{\bar{\bar{M}}}\right) f_a^1 f_a^2 \varepsilon_a \left(\frac{r_a^1 - r_a^2}{\bar{r}_a}\right)^2}{\sum_{a=1}^{n} c_a} \tag{S2}$$

$$\bar{M}_a = \sum_k f_a^k M_a^k \tag{S3}$$

$$\bar{r}_a = \sum_k f_a^k r_a^k \tag{S4}$$

$$\Gamma = \Gamma_{mass} + \Gamma_s = \frac{1}{4}\left(\frac{\bar{M}_1}{\bar{\bar{M}}}\right)^2 x(1-x)\left[\left(\frac{M_1^1 - M_1^2}{\bar{M}_1}\right)^2 + \varepsilon_1 \left(\frac{r_1^1 - r_1^2}{\bar{r}_1}\right)^2\right] \tag{S5}$$

where n is the number of different crystallographic sublattice types in the lattice and c_a is the relative degeneracy of the respective site. For $CuFeS_2$, the parameter values can be obtained with: the Cu site, the Fe site, and the S site. So n=3 and c_1=c_2=1, c_3=2. $\bar{\bar{M}}$ is the average atomic mass of compound. $\bar{M}_a$ and $\bar{r}_a$ are the average mass and radius on the a_{th} sublattice, respectively. f_a^k is fractional occupation of the kth atoms on the a_{th} sublattice. M_a^k and r_a^k are the atomic mass and redius, respectively.

Theoretical calculation of Debye model[3, 4]:

$$k_l = \frac{k_b}{\hbar} T^3 \int_0^{\theta/T} \frac{x^4 e^x}{\tau^{-1}(e^x - 1)^2} dx \tag{S6}$$

where $x = \hbar\omega / k_B T$, x is the phonon frequency, k_B is the Boltzmann constant, $\hbar$ is the reduced Planck constant, θ is the Debye temperature (263 K), v is the velocity of sound (2938 m s^{-1}), and τ is the phonon scattering relaxation time. The overall phonon

scattering relaxation rate τ is written as:

The overall phonon scattering relaxation rate τ is written as:

$$\tau^{-1} = \tau_U^{-1} + \tau_{GB}^{-1} + \tau_{PD}^{-1} \tag{S7}$$

where τ_U is the relaxation time of Umklapp processes:

$$\tau_U^{-1} = A_N \frac{\hbar\gamma^2}{Mv^2\theta_D}\omega^2 T exp(-\frac{\theta_D}{3T}) \tag{S8}$$

τ_{GB} is relaxation time of grain boundary (or precipitate) scattering:

$$\tau_{GB}^{-1} = v/d \tag{S9}$$

τ_{PD} is point defects scattering :

$$\tau_{PD}^{-1} = \frac{V\omega^4}{4\pi v^3}\Gamma \tag{S10}$$

M is the molar mass, v is the average phonon group velocity, d is the grain (or precipitate) size, θ_D is the Debye temperature, A_N is an additional factor induced by Normal process, Γ is the scattering parameter.

Single Parabolic Band Model[5]:

The bands of semiconductor usually are described with parabolic simply, which can easily estimate the performance based on a small number of parameters and tests. According the tested data of carrier concentration and *S*, the Pisarenko lines can be estimated based on equations S10-S13:

$$S = \pm \frac{k_B}{e}(\frac{2F_1(\eta))}{F_0(\eta))} - \eta) \tag{S11}$$

$$r_H = \frac{3F_{1/2}(\eta)F_{-1/2}(\eta)}{2F_0^2(\eta)} \tag{S12}$$

$$F_n(\eta) = \int_0^\infty \frac{\chi^n}{1 + e^{\chi - \eta}} d\chi \tag{S13}$$

$$m^* = \frac{h^2}{2k_B T}\left[\frac{n \cdot r_H}{4\pi F_{1/2}(\eta)}\right]^{2/3} \tag{S14}$$

where $F_n(\eta)$ is the *n*th order Fermi integral, η the reduced Fermi energy, r_H is the Hall factor, h is the Planck constant, k_B is the Boltzmann constant, and m^* is the total density

of states effective mass.

References:

1. H. Xie, X. Su, G. Zheng, T. Zhu, K. Yin, Y. Yan, C. Uher, M. G. Kanatzidis and X. Tang, *Adv. Energy Mater.*, 2017, **7**, 1601299.
2. Y. Li, T. Zhang, Y. Qin, T. Day, G. Jeffrey Snyder, X. Shi and L. Chen, *J. Appl. Phys.*, 2014, **116**, 203705.
3. C. Zhou, Z. Shi, B. Ge, K. Wang, D. Zhang, G. Liu and G. Qiao, *J. Mater. Chem. A.*, 2017, **5**, 2876-2884.
4. J. P. Heremans, V. Jovovic, E. S. Toberer, A. Saramat, K. Kurosaki, A. Charoenphakdee, S. Yamanaka and G. J. Snyder, *Science*, 2008, **321**, 554-557.
5. Z. Liu, H. Geng, J. Mao, S. Jing, R. He, C. Wang, W. Cai, J. Sui and Z. Ren, *J. Mater. Chem. A.*, 2016, **4**, 16834-16840.